Site Amplifications for Generic Rock Sites

by

David M. Boore and William B. Joyner

ABSTRACT

Seismic shear-wave velocity as a function of depth for generic rock sites has been estimated from borehole data and studies of crustal velocities, and this velocity has been used to compute frequency-dependent amplifications for zero attenuation for use in simulations of strong ground motion. We define a generic rock site as one whose velocity at shallow depths equals the average of those from the rock sites sampled by the borehole data. Most of the boreholes are in populated areas and for that reason the rock sites sampled are of particular engineering significance. The amplifications on rock sites sampled by the boreholes can be in excess of 3.5 at high frequencies, in contrast to the amplifications of less than 1.2 expected on very hard rock sites. The consideration of unattenuated amplification alone is computationally convenient, but what matters for ground-motion estimation is the combined effect of amplification and attenuation. For reasonable values of the attenuation parameter κ_0, the combined effect of attenuation and amplification for rock sites peaks between about 2 to 5 Hz with a maximum level of less than 1.8. The combined effect is about a factor of 1.5 at 1 Hz and is less than unity for frequencies in the range of 10 to 20 Hz (depending on κ_0).

The borehole data yield shear-wave velocities ($\overline{V}_{30}$) of 618 and 306 m/s for "rock" and "soil" sites, respectively, when averaged over the upper 30 m. From this, we recommend that $\overline{V}_{30}$ equals 620 and 310 m/s for applications requiring the average velocity for "rock" and "soil" sites in western North America.

By combining the amplifications for rock sites and the site factors obtained from our analysis of strong-motion data, we derive amplifications for sites with $\overline{V}_{30}$ = 520 m/s (NEHRP Class C, corresponding to a mix of rock and soil sites) and $\overline{V}_{30}$ = 310 and 255 m/s (average soil and NEHRP Class D sites, respectively). For the average soil site the combined effect of amplification and attenuation exceeds a factor of 2.0 for frequencies between 0.4 and about 4 Hz, with a peak site effect of 2.4; the peak of the NEHRP Class D site effect is 2.7.

This paper is a shortened version of a recently published paper (Boore and Joyner, 1997).

KEYWORDS: Earthquakes; frequency; seismic shear-wave velocity; site amplification.

1. INTRODUCTION

Simulations of ground motions are often needed on rock sites, e.g., for use in seismic analysis and design of structural systems and in building codes. As is the case for soil sites, not all rock sites are created equal (e.g., Steidl *et al.*, 1996), and for site-specific applications the properties of the local site should be used

in the simulations. In many cases, however, it is sufficient to do the simulations for a representative or generic rock site. The main purpose of this paper is to present average velocity vs. depth and amplification vs. frequency for such sites. The amplifications can be used directly in the stochastic model for simulating earthquake ground motions (e.g., Boore, 1996).

The amplifications are based on shear velocity and density as functions of depth. The first task in the paper is to obtain a profile of shear-wave velocity vs. depth. To do this we use an extensive set of shear-wave travel-time measurements made in boreholes to constrain the shallow velocities, and we use studies of *P*-wave velocities in the crust as a guide for choosing the deeper velocities. The next task is to compute the amplifications; for this we use the quarter-wavelength approximation introduced by Joyner *et al.* (1981). The approximation is checked using wave propagation to calculate the exact response of the velocity structure used in the quarter-wavelength approximation.

2. VELOCITY AND DENSITY STRUCTURE

The travel time of *S* waves (S_{tt}) from the surface to any depth below a site is the fundamental property needed for the determination of the amplification (velocities, of course, can also be determined from S_{tt}). These travel times are available from downhole surveys made in boreholes, and can be used to estimate directly the amplification at high frequencies. We have entered all the S_{tt} from over 210 boreholes logged over the past 20 years by J. Gibbs, T. Fumal, and colleagues (Fumal *et al.*, 1981, 1982a, 1982b, 1984; Gibbs, 1989; Gibbs *et al.*, 1975, 1976, 1977, 1980, 1990, 1992, 1993, 1994a, 1994b; Gibbs and Fumal, 1994); in addition, we have added data from a few other published studies (Fletcher *et al.*, 1990; Thiel and Schneider, 1993) and from several unpublished studies (written communications from J. Gibbs, 1995 and T. Fumal, 1996). We then assigned a "rock" or "soil" classification to each borehole, based on surficial geology, following Joyner and Boore's (1981) scheme that "rock" sites are those described by terms such as "granite", "diorite", "gneiss", "chert", "graywacke", "limestone", "sandstone", or "siltstone", as long as the rock is overlain by less than 4 to 5 meters of soils. The distribution of shear velocity averaged over the upper 30 m (most of the holes were 30 m or shallower) is shown in Figure 1 for the two subsets of the borehole database. In the subsequent analysis we use only the data from 57 "rock" boreholes.

The borehole data are increasingly scarce at depth greater than 30 m, and for this reason our velocity function is constructed by using the borehole results to determine the best average shallow velocity, and then using *P*-wave velocities in the crust based on velocity surveys and earthquake location studies to estimate deeper *S*-wave velocities on the assumption that Poisson's ratio is close to 0.25 at depths in excess of several kilometers. We patch together the shallow and deeper velocity functions in order to obtain a continuous velocity-depth function.

The shallow velocity is obtained by interpolating the observed times in boreholes at 2 m intervals from the surface to the deepest recording in each hole, averaging S_{tt} at each depth for which at least two interpolated values are available, fitting a functional form to the average S_{tt} as a function of depth, and

converting this average travel time into a velocity-depth function. Figure 2 shows the individual travel times, the geometrically averaged travel times, a power-law fit to the averages (determined using unweighted least-squares) between 0 and 30 m, and the number of data points for each depth. Straightforward differentiation of the travel-time function (see Figure 2) yields the following equation for the shear velocity:

$$\beta(z) = 2.206\ z^{0.272} \qquad (1)$$

with the units of β and z being km/s and km, respectively. The power-law functional form was chosen after trials with several other forms. It has the advantage of providing a simple relation between travel time and velocity and a good fit to the observations, but it has the obvious disadvantage of predicting zero velocity at the surface. The value at 1 m depth (337 m/s) is reasonable. We replace the velocity between 0 and 1 m depth with a constant-velocity layer such that the travel time to 1 m equals that given by the power-law fit. The influence of these shallow depths on the amplification is only at very high frequencies (in excess of 30 Hz), however, and, as shown later, attenuation will severely blunt the amplification at these frequencies. We use equation (1) for the shear-wave velocity between 0.001 and 0.03 km.

Because of a lack of data, it is difficult to constrain the shear-wave velocity at greater depths. At depths below 4 km we estimate shear-wave velocity from compressional velocities, assuming a constant Poisson's ratio of 0.25. We chose 4 km because the lithostatic pressure at this depth is about 1 kbar, the pressure at which most cracks should be closed and below which Poisson's ratio should be near 0.25 for the crustal rocks of concern to us (e.g., Clark, 1966; Christensen and Mooney, 1995; Christensen, 1996). There is good evidence that Poisson's ratio is not constant at shallower depths (e.g., Nicholson and Simpson, 1985), and for this reason we cannot directly use the numerous measurements of crustal *P*-wave velocities obtained from refraction experiments and from earthquake location investigations to obtain *S*-wave velocities for depths less than 4 km. Representative *P*-wave velocity profiles are shown in Figure 3. We adjusted the parameters of a power-law functional form to roughly agree with the measured *P*-wave results below 4 km and converted this to a function giving *S*-wave velocity by dividing the *P*-wave velocities by $\sqrt{3}$. Our function is indicated by the heavy line in Figure 3.

We patch together the velocities at depths less than 0.03 km (from boreholes) and greater than 4 km (from *P*-waves) with two power law functions. In doing this we were guided by the *P*-wave velocities near 3.7 km/s at 0.2 km depth for Franciscan rocks on either side of the southern San Francisco Bay (Hazlewood and Joyner, 1973; Hazlewood, 1974). For Poisson's ratio of 0.25, this *P*-wave velocity yields an *S*-wave velocity of 2.1 km/s; we consider this an upper bound and therefore constrained the velocity function to pass through a smaller value at a depth of 0.2 km. Our final velocity model is plotted in Figure 4.

The density is given as a function of shear velocity by the simple relation

$$\rho(z) = 2.5 + (\beta(z) - 0.3) \times \frac{(2.8-2.5)}{(3.5-0.3)}$$

with ρ in gm/cc and β in km/s. Equation (2)

is a simple interpolation of end point values chosen by referring to various reference books and from personal experience of one of the authors (WBJ) in measuring densities; it is only to be used for shear velocities between 0.3 and 3.5 km/s. A density of 2.5 gm/cc was assigned to velocities less than 0.3 km/s.

3. 30 m TIME-AVERAGED VELOCITY FOR "ROCK" AND "SOIL" SITES

A site measure of importance in predicting ground shaking and in building codes (e.g., Boore *et al.*, 1994; Borcherdt, 1994; Midorikawa *et al.*, 1994) is the time-averaged shear-wave velocity from the surface to 30 m depth $\overline{V}_{30} = 30/S_{tt}(30\text{ m})$, where the units of $\overline{V}_{30}$ are m/s). The travel time curve fit to the data in Figure 2 yields an average velocity of 618 m/s; a similar analysis for the "soil" subset of the borehole database yields 306 m/s. Based on these results, we suggest that average "rock" and "soil" sites in western North America correspond to average velocities of 620 and 310 m/s, respectively. These numbers can be used to compare ground-motion attenuation equations base on "rock" and "soil" site classifications with those that use $\overline{V}_{30}$ to characterize the geology at a site.

4. THE QUARTER-WAVELENGTH APPROXIMATION

The quarter-wavelength approximation for computing site amplification was introduced by Joyner *et al.* (1981). For a particular frequency the amplification is given by the square root of the ratio between the seismic impedance (velocity times density) averaged over a depth corresponding to a quarter wavelength and the seismic impedance at the depth of the source (as used here, the averages of the seismic velocity and density are determined separately instead of their product being averaged; this should make little difference in the results). The approximation is relatively insensitive to discontinuities in seismic velocity; the method does not produce the peaks and valleys due to the interference of multiply-reflected waves. We consider this lack of resonant effects to be an advantage if, as in this paper, an amplification function insensitive to the details in the layering is desired.

Comparisons of the approximate and exact theoretical amplifications include those of Boore and Joyner (1991), Boatwright (personal commun., 1987), and Silva and Darragh (1995); we include another comparison in this paper. The available comparisons suggest that the quarter-wavelength approximation provides a good estimate of the mean values of the response.

The algorithm is the following: the S travel time ($S_{tt}(z)$) from the surface to depth z is either taken from downhole surveys or is computed using shear velocity as a function of depth; the average velocity to depth z, $\overline{\beta}(z)$, is $z/S_{tt}(z)$ and the frequency corresponding to the depth, $f(z)$, is 1/(4 times $S_{tt}(z)$); a travel-time-weighted average is taken of the density, $\overline{\rho}(z)$; and the amplification ($A(f)$) is given by

$$A(f(z)) = \sqrt{\rho_s \beta_s / \overline{\rho}(z)\overline{\beta}(z)}, \qquad (3)$$

where the subscript s represents values in the vicinity of the source.

When we refer to amplification, we mean the Fourier amplitude spectrum of the surface motion produced for **unattenuated** incident

plane waves divided by the Fourier amplitude spectrum that would have been recorded at the surface of a uniform halfspace by the same incident planewaves (the amplification therefore approaches unity for very long-period waves). Of course, the site response of interest includes attenuation, but we have considered the amplification and attenuation separately because we prefer to parameterize the attenuation by the operator $\exp(-\pi \kappa_0 f)$. By so doing, it is natural in computer simulations to treat the amplification
and attenuation as separate entities, though this distinction may be somewhat artificial. A careful study of the response of a particular site to seismic waves should include attenuation as a point property with depth. Even then it is important to recognize that using a parameter such as Q to represent the attenuation is only a phenomenological description of a complex process involving intrinsic and scattering attenuation mechanisms.

5. AMPLIFICATION FROM VELOCITY AND DENSITY PROFILES

We use the velocity and density functions to compute amplifications, using the quarter-wavelength approximation, and assuming that the velocity near the source is close to the velocity in our model at 8 km depth (the amplifications are only sensitive to variations of several km in this source depth for frequencies less than 0.1 Hz). The computations were made by program *Site_Amp* (Boore, 1996). The results are shown in Figure 5. The amplification for rock sites increases from near 1 at 0.1 Hz to over 3 for frequencies greater than about 12 Hz.

In order to check the quarter-wavelength assumption, the velocity model was replaced with one consisting of a stack of constant-velocity layers (such that the travel time to each interface in the stack was the same as in the continuous velocity model), and the amplification was computed using the propagator-matrix method of Haskell (1960), as implemented by C. Mueller's program *Rattle*for *SH* waves. (A Q of 10,000 in each layer was used to simulate no attenuation.) Because the base of the velocity model is at 8 km in high-velocity material, incidence angles of 30 and 45 degrees were used to approximate the range of angles that would exist for events not directly under the site (the incidence angles would be smaller for input at shallower depths because of refraction). The amplifications are shown in Figure 5. The oscillations at high frequencies are due to the finite thickness of the layering (1 m for the first two layers and 2 m to depths of 0.2 km). The quarter-wavelength approximation is a good representation of the overall amplification; it has the advantages of being insensitive to the layering in the system, taking little computation time, and allowing back-of-the-envelope estimates of the amplification and the depths affecting various frequencies of motion.

As discussed earlier, we choose to separate amplification and near-site attenuation for ease in incorporating the two effects in our computer codes for calculating ground motions; what counts for ground motions, of course, is the combined effect of amplification and attenuation. Figure 6 shows this combined effect for a range of values of the attenuation parameter κ_0 found by Silva and Darragh (1995) for rock sites in western North America (the amplification factors of Boore, 1986, were used to obtain these estimates). For reasonable values of κ_0 (i.e., in excess of

0.01 for most rock sites in western North America, although an average value of 0.005 was obtained by Hough *et al.*, 1988, on granitic rocks in the Anza region of southern California), the large amplifications at high frequencies are much reduced by the attenuation. It is important to note, however, that the overall effect of the amplification and attenuation is still larger than unity over a wide range of frequencies of engineering interest.

The quarter-wavelength approximation makes it easy to answer the question of what depth influences what frequency. The relationship between depth and frequency is shown in Figure 7 for our rock model. This figure shows that frequencies as low as 1 Hz are influenced by velocities in the upper few hundred meters of the Earth at rock sites. At soil sites the primary influence on 1 Hz amplification would be at even shallower depths. The velocity models used in the calculation of wave propagation in layered media should have near-surface velocities that are commensurate with the frequencies of the calculated motions. We fear that a number of seismologists use models with near-surface shear-wave velocities that are too high, thinking that the near-surface layers can be neglected without realizing that although the thickness is small, the travel time through the layers is not small.

6. AMPLIFICATIONS FOR OTHER SITE CLASSES

It is useful to obtain amplification functions for sites other than the very hard rock and rock sites. Rather than repeat the analysis of this paper for boreholes falling into other classes, we use a combination of the rock amplification shown in Figure 5 and the empirical results of Boore *et al.* (1994) in which response spectra are given as a function of $\overline{V}_{30}$. Our scheme is simple: we use the ratio of response spectra computed from Boore et al. (1994) for sites with $\overline{V}_{30} = 620$ m/s and V_{30} equal to the desired velocity as a correction factor applied to the rock amplifications. We used subjective judgment to extend the correction factors to frequencies outside the range used by Boore *et al.* (1994). The procedure assumes that the ratio of Fourier and response spectra are the same. This is not strictly true, particularly at frequencies higher than about 8 Hz. We fine tune the amplifications by generating simulated response spectra for the desired $\overline{V}_{30}$ and comparing them with the empirical response spectra of Boore *et al.* (1994). Ratios of the spectra for various frequencies are used in an iterative procedure to adjust the amplifications. We chose three site classes: the NEHRP building code classes C and D (BSSC, 1994) and the average soil class. $\overline{V}_{30}$ for the two NEHRP classes (520 and 255 m/s) are given by the geometrical means of the velocities defining the boundaries of each class. The velocity for an average soil site (310 m/s) was discussed in the previous section.

We show the combined effect of amplification and attenuation in Figure 8. The site effect for the soil sites exceeds a factor of 2 over a wide range of frequencies of importance in engineering. The attenuation parameter κ_0 was held fixed at 0.035 s in the derivation of the amplifications. Consistent results can also be obtained for other values of κ_0 as long as the amplification is adjusted by the factor $\exp(-\pi(\kappa_0 - \kappa_{new})f)$.

7. CONCLUSIONS AND DISCUSSION

Using borehole data and studies of crustal velocities, we have estimated seismic shear-wave velocity and density as a function of depth for rock sites such as are found in many tectonically active regions, with an average $\overline{V}_{30}$ of 620 m/s. From the shear-wave velocity and density vs. depth functions we produce amplifications as a function of frequency for use in simulations of strong ground motion. The amplifications are in excess of 3.5 at high frequencies. Attenuation, however, will reduce these amplifications such that the combined effect for the rock sites might have a maximum of about a factor of 1.8 for $\kappa_0 = 0.02$ s and 1.5 for $\kappa_0 = 0.04$ s. The scatter in the amplifications computed for individual boreholes is considerable, suggesting that the mean amplifications proposed in this paper should be used with caution for site-specific studies. The large variation in site response for rock sites has also been emphasized by Schneider and Silva (1994).

We also find from the analysis of borehole data that average "rock" and "soil" sites are characterized by time-averaged shear-wave velocities in the upper 30 m of 620 and 310 m/s, respectively.

Although we have treated them separately, there may be a correlation between the attenuation parameter κ_0 and $\overline{V}_{30}$. This is certainly the case in going from very hard rock, for which κ_0 is often less than 0.01 s (e.g., Atkinson, 1996), to ordinary rock, for which we and others find representative values near 0.04 s for κ_0. There may also be a tendency within the generic rock category for κ_0 to decrease with increasing $\overline{V}_{30}$ (W. Silva, written commun., 1995). Correlations between κ_0 and $\overline{V}_{30}$, however, might depend on geographic region and class of geologic materials beneath a site. κ_0 is affected by more of the travel path than the part contributing to the amplification (Anderson et al., 1996). For this reason two sites with the same V_{30} could have different values of κ_0 (as has been found by Atkinson, 1996, for very hard rock sites in southeastern and southwestern Canada, with κ_0 being less than 0.004 for sites in the former region and 0.011 for sites in the latter region). In addition, the correlation between κ_0 and $\overline{V}_{30}$ is probably different for rock and for soils. We expect that near-surface velocity gradients in soils would be less than in rocks and that scattering would be less important in soils. For these reasons, the amplification function and κ_0 might be different for two sites with the same $\overline{V}_{30}$.

Although our primary reason for separating the effects of amplification and attenuation is for convenience in providing input parameters for our computer codes for estimating ground shaking, we note that measurements of κ_0 from data also use a similar separation. Any measurement of κ_0 is tied to the amplification. In most cases of measurements of κ_0, however, the amplification is implicitly assumed to be unity, or at least independent of frequency over the range used in determining κ_0, a result that the borehole data suggests is unlikely to be true. The high-frequency dependence of the amplification is critically dependent on the gradient of the velocity with depth near the surface (e.g., less than 10 m for $f > 10$ Hz, according to Figure 7). In order for the rock amplifications to flatten for frequencies greater than 10 Hz, however, the gradient in the upper 10 m would have to be replaced by a constant velocity layer. The borehole data in Figure 2 argues against this,

at least for rock sites. If κ_0 is independent of frequency, then in principle it should be possible to distinguish between a site with constant amplification at high frequency and one with increasing amplification: a plot of the log of the spectrum vs. linear frequency will approach a straight line in the former case, while an increasing amplification will lead to curvature of the high-frequency part of the spectrum. To study this, we replotted Figure 6 using log, linear axes. The curvature was very hard to see, and would be completely obscured for real, noisy data. On the other hand, determinations of κ_0 by fitting a straight line to log spectrum vs. frequency (Anderson and Hough, 1984) yields estimates near 0.034 for the case when κ_0 is 0.040. Therefore, as expected, measurements of κ_0 which do not account for increasing amplification with frequency will be lower than measurements that account for the amplification. Caution must be used in comparing values of κ_0 from various studies; it is necessary to consider what, if any, account has been taken of amplification of the spectrum.

As the example above illustrates, derived parameters are dependent on the assumptions embedded in the underlying model, a point that we fear is often overlooked. Another example is in the estimation of seismic moments of small earthquakes at rock sites, which are usually determined with no regard for the amplifications that can occur due to the decrease in seismic velocities near the Earth's surface; Figure 6 suggests that such determinations might be systematically high by a factor of about 1.4 for many rock sites (those with $\overline{V}_{30}$ considerably less than several km/s) if computed from waves with frequencies of 1 Hz. The factor would be more than 1.4 for soil sites.

The rock amplifications have been modified to obtain amplification factors that are appropriate for sites classified by average shear-wave velocities $\overline{V}_{30}$ equal to 520, 310, and 255 m/s. These site classes correspond to NEHRP class C, average soil, and NEHRP class D, respectively. The combined effect of the amplification and attenuation reaches a factor of 2.7 for $\overline{V}_{30} = 255$ m/s and exceeds a factor of 2 for a wide range of frequencies of engineering interest.

We stress the obvious point that rock sites on which strong motions have been recorded are not underlain by uniform half spaces; our analysis of borehole data finds a strong gradient with depth, presumably due to weathering processes and open fractures. It would be a mistake, however, to assume that the same gradients apply to the rock beneath soil sites. If rock recordings are to be used as input to a soil column, then these rock recordings should first be deconvolved to a depth where the velocity profile is comparable to the rock beneath the soil column (that depth could be 1 km or more), before being convolved with the response of the rock between that depth and the base of the soil column. This is a site-specific matter and requires the determination of shear velocity to sufficient depths, both beneath the rock recording and beneath the soil column.

8. ACKNOWLEDGMENTS

We thank Jim Gibbs for helping enter the borehole data and Charles Mueller for use of his program *Rattle*. Jim Gibbs and Tom Fumal provided unpublished travel-time data for two boreholes, and Joe Fletcher supplied computer files of S_{tt} for several rock sites in southern California (Keenwild and Pinyon Flat). Harold Magistrale provided velocity

and density profiles for a few locations, also in southern California. We also thank Rachel Abercrombie, Peter Malin, and Tom McEvilly for data and information about the Cajon Pass, Parkfield area, and Oroville boreholes. We are grateful to Walt Silva for his discussions and comments and to Mehmet Celebi and Roger Borcherdt for their thoughtful reviews of the manuscript. This work was partially supported by the U.S. Nuclear Regulatory Commission.

9. REFERENCES

Anderson, J. G. and S. E. Hough (1984). A model for the shape of the Fourier amplitude spectrum of acceleration at high frequencies, *Bull. Seism. Soc. Am.* **74**, 1969-1993.

Anderson, J.G., Y. Lee, Y. Zeng, and S. Day (1996). Control of strong motion by the upper 30 meters, *Bull. Seism. Soc. Am.* **86**, 1749-1759.

Atkinson, G.M. (1996). The high-frequency shape of the source spectrum for earthquakes in eastern and western Canada, *Bull. Seism. Soc. Am.* **86**, 106-112.

Boore, D. M. (1986). Short-period *P*- and *S*-wave radiation from large earthquakes: implications for spectral scaling relations, *Bull. Seism. Soc. Am.* **76**, 43-64.

Boore, D.M. (1996). SMSIM -- Fortran programs for simulating ground motions from earthquakes: version 1.0, *U.S. Geol. Survey Open-File Rept. 96-80-A, 96-80-B*, 69 p.

Boore, D.M. and W.B. Joyner (1991). Estimation of ground motion at deep-soil sites in eastern North America, *Bull. Seism. Soc. Am.* **81**, 2167-2185.

Boore, D.M. and W.B. Joyner (1997). Site amplifications for generic rock sites, *Bull. Seism. Soc. Am.* **87**, (in press).

Boore, D.M., W.B. Joyner, and T.E. Fumal (1994). Estimation of response spectra and peak accelerations from western North American earthquakes: An interim report, Part 2 *U.S. Geol. Survey Open-File Rept. 94-127*, 40 pp.

Borcherdt, R.D. (1994). Estimates of site-dependent response spectra for design (methodology and justification), *Earthquake Spectra* **10**, 617-653.

Building Seismic Safety Council (BSSC) (1994). NEHRP recommended provisions for seismic regulations for new buildings, Part 1 - Provisions, FEMA 222A, Federal Emergency Management Agency, 290 p.

Christensen, N.I. (1996). Poisson's ratio and crustal seismology, *J. Geophys. Res.* **101**, 3139-3156.

Christensen, N.I. and W.D. Mooney (1995). Seismic velocity structure and composition of the continental crust: A global view, *J. Geophys. Res.* **100**, 9761-9788.

Clark, S.P., Jr. (Editor) (1966). *Handbook of Physical Constants*, Geological Society of America Memoir 97, 587 p.

Fletcher, J.B., T. Fumal, H.-P. Liu, and L.C. Carroll (1990). Near-surface velocities and attenuation at two boreholes near Anza, California, from logging data, *Bull. Seism. Soc. Am.* **80**, 807-831.

Fumal, T.E. (1978). Correlations between seismic wave velocities and physical

properties of near-surface geologic materials in the southern San Francisco Bay region, California, *U.S. Geol. Survey Open-File Rept. 78-1067*, 114 p.

Fumal, T.E., J.F. Gibbs, and E.F. Roth (1981). In-situ measurements of seismic velocity at 19 locations in the Los Angeles, California region, *U.S. Geol. Survey Open-File Rept. 81-399*, 121 p.

Fumal, T.E., J.F. Gibbs, and E.F. Roth (1982a). In-situ measurements of seismic velocity at 10 strong motion accelerograph stations in central California, *U.S. Geol. Survey Open-File Rept. 82-407*, 76 p.

Fumal, T.E., J.F. Gibbs, and E.F. Roth (1982b). In-situ measurements of seismic velocity at 22 locations in the Los Angeles, California region, *U.S. Geol. Survey Open-File Rept. 82-833*, 138 p.

Fumal, T.E., J.F. Gibbs, and E.F. Roth (1984). In-situ measurements of seismic velocity at 16 locations in the Los Angeles, California region, *U.S. Geol. Survey Open-File Rept. 84-681*, 109 p.

Gibbs, J.F. (1989). Near-surface *P*- and *S*-wave velocities from borehole measurements near Lake Hemet, California, *U.S. Geol. Survey Open-File Rept. 89-630.*

Gibbs, J.F. and T.E. Fumal (1994). Seismic velocities and geologic logs from borehole measurements at seven strong-motion stations that recorded the 1989 Loma Prieta, California, earthquake, Part IV, *U.S. Geol. Survey Open-File Rept. 94-552*, 89 p.

Gibbs, J.F., T.E. Fumal, and R.D. Borcherdt (1975). In-situ measurements of seismic velocities at twelve locations in the San Francisco Bay region, *U.S. Geol. Survey Open-File Rept. 75-564*, 87 p.

Gibbs, J.F., T.E. Fumal, and R.D. Borcherdt (1976). In-situ measurements of seismic velocities in the San Francisco Bay region...Part II, *U.S. Geol. Survey Open-File Rept. 76-731*, 145 p.

Gibbs, J.F., T.E. Fumal, and R.D. Borcherdt (1977). In-situ measurements of seismic velocities in the San Francisco Bay region...Part III, *U.S. Geol. Survey Open-File Rept. 77-850*, 143 p.

Gibbs, J.F., T.E. Fumal, and E.F. Roth (1980). In-situ measurements of seismic velocity at 27 locations in the Los Angeles, California region, *U.S. Geol. Survey Open-File Rept. 80-378*, 167 p.

Gibbs, J.F., E.F. Roth, T.E. Fumal, N.A. Jasek, and M.A. Emslie (1990). Seismic velocities from borehole measurements at four locations along a fifty-kilometer section of the San Andreas fault near Parkfield, California, *U.S. Geol. Survey Open-File Rept. 90-248*, 35 p.

Gibbs, J.F., T.E. Fumal, D.M. Boore, and W.B. Joyner (1992). Seismic velocities and geologic logs from borehole measurements at seven strong-motion stations that recorded the Loma Prieta earthquake, *U.S. Geol. Survey Open-File Rept. 92-287*, 139 p.

Gibbs, J.F., T.E. Fumal, and T.J. Powers (1993). Seismic velocities and geologic logs from borehole measurements at eight strong-motion stations that recorded the 1989 Loma Prieta, California, earthquake, *U.S. Geol. Survey Open-File Rept. 93-376*, 119 p.

Gibbs, J.F., T.E. Fumal, and T.J. Powers (1994a). Seismic velocities and geologic logs from borehole measurements at seven strong-motion stations that recorded the 1989 Loma Prieta, California, earthquake, *U.S. Geol. Survey Open-File Rept. 94-222*, 104 p.

Gibbs, J.F., T.E. Fumal, R.D. Borcherdt, R.E. Warrick, H.-P. Liu, and R.E. Westerlund (1994b). Seismic velocities and geologic logs from boreholes at three downhole arrays in San Francisco, California, *U.S. Geol. Survey Open-File Rept. 94-706*, 40 p.

Hadley, D. and H. Kanamori (1977). Seismic structure of the Transverse Ranges, California, *Geol. Soc. Am. Bull.*, **88**, 1469-1478.

Haskell, N.A. (1960). Crustal reflection of plane *SH* waves, *J. Geophys. Res.* **65**, 4147-4150.

Hauksson, E. (1987). Seismotectonics of the Newport-Inglewood fault zone in the Los Angeles basin, southern California, *Bull. Seism. Soc. Am.* **77**, 539-561.

Hauksson, E. and L.M. Jones (1988). The July 1986 Oceanside (M_L = 5.3) earthquake sequence in the continental borderland, southern California, *Bull. Seism. Soc. Am.* **78**, 1885-1906.

Hazlewood, R.M. (1974). Preliminary report of seismic refraction survey along the east side of the San Francisco Bay, Alameda County, California, *U.S. Geol. Survey Open-File Rept.*, 10p.

Hazlewood, R.M. and W.B. Joyner (1973). Preliminary report of seismic refraction survey, Redwood Shores, San Mateo County, California, *U.S. Geol. Survey Open-File Rept.*, 9p.

Hough, S. E., J. G. Anderson, J. Brune, F. Vernon III, J. Berger, J. Fletcher, L. Haar, T. Hanks, and L. Baker (1988). Attenuation Near Anza, California, *Bull. Seism. Soc. Am.* **78**, 672-691.

Joyner, W.B., R.E. Warrick, and T.E. Fumal (1981). The effect of Quaternary alluvium on strong ground motion in the Coyote Lake, California, earthquake of 1979, *Bull. Seism. Soc. Am.* **71**, 1333-1349.

Magistrale, H., K. McLaughlin, and S. Day (1996). A geology-based 3D velocity model of the Los Angeles basin sediments, *Bull. Seism. Soc. Am.* **86**, 1161-1166.

Midorikawa, S., M. Matsuoka, and K. Sakugawa (1994). Site effects on strong-motion records observed during the 1987 Chiba-Ken-Toho-Oki, Japan earthquake, *Proc. 9th Japan Earthq. Eng. Symp.* **3**, E085-E090.

Nicholson, C. and D.W. Simpson (1985). Changes in V_p/V_s with depth: Implications for appropriate velocity models, improved earthquake locations, and material properties of the upper crust, *Bull. Seism. Soc. Am.* **75**, 1105-1123.

Schneider, J.F. and W.J. Silva (1944). What is rock? Implications for site response estimation (abs.), *Seism. Res. Lett.* **65**, 44.

Silva, W. J., and R. B. Darragh (1995). Engineering Characterization of Strong Ground Motion Recorded at Rock Sites, Electric Power Research Institute, Palo Alto, Calif., Report No. TR-102262.

Steidl, J.H., A.G. Tumarkin, and R.J. Archuleta (1996). What is a reference site?, *Bull. Seism. Soc. Am.* **86**, 1733-1748.

Thiel Jr., C. C. and J. F. Schneider (1993). Investigations of Thirty-Three Loma Prieta Earthquake Strong Motion Recording Sites, final report of project sponsored by the Building Contractors Society of Japan and the Electric Power Research Institute, California Universities for Research in Earthquake Engineering (CUREe), Dept. of Civil Engineering, Stanford Univ., Stanford, Calif.

Wald, D.J., D.V. Helmberger, and T.H. Heaton (1991). Rupture model of the 1989 Loma Prieta earthquake from the inversion of strong-motion and broadband teleseismic data, *Bull. Seism. Soc. Am.* **81**, 1540-1572.

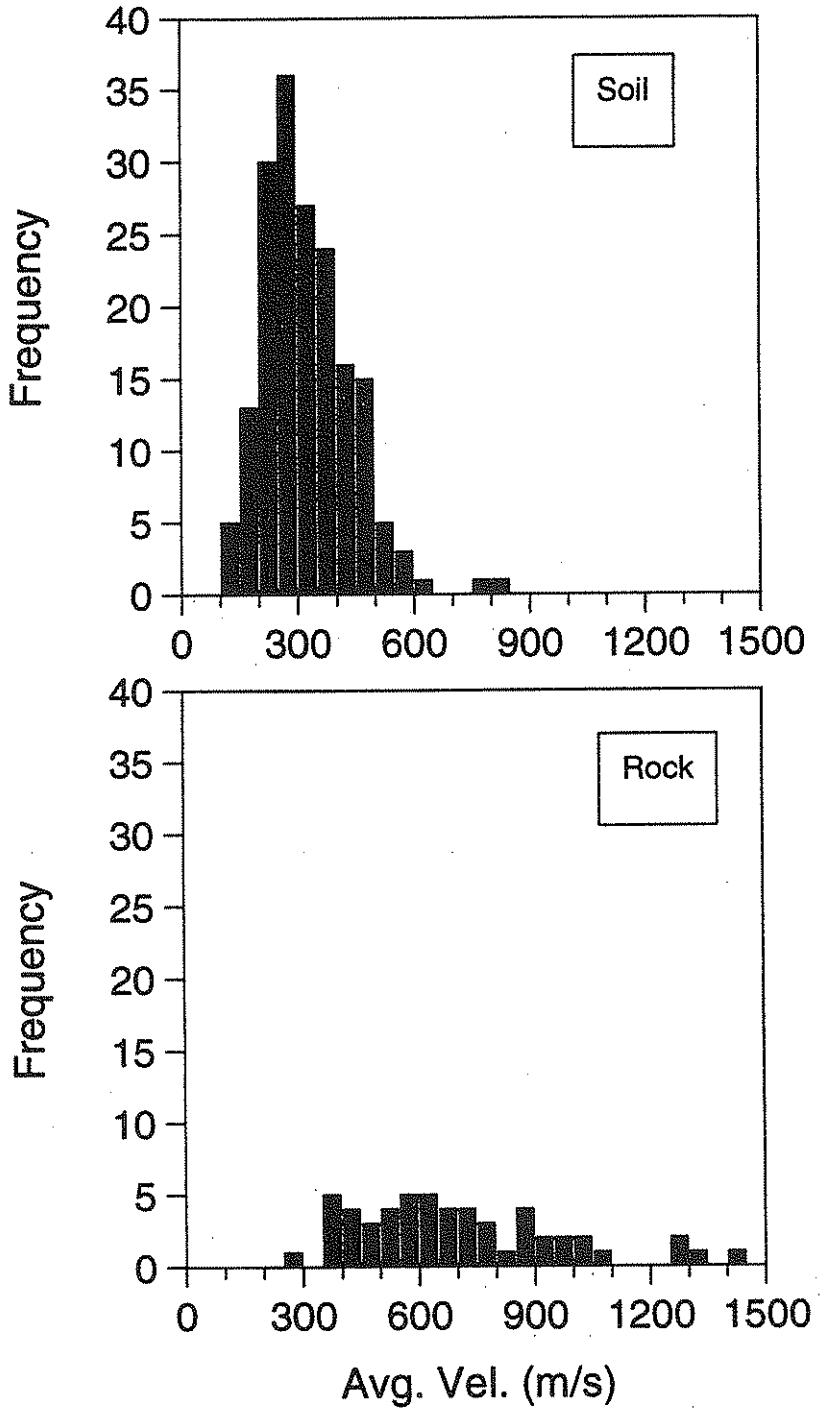

Figure 1. Histograms of shear velocity averaged over the upper 30m, from downhole surveys in boreholes. Many of the boreholes did not quite reach 30m, and for the sake of estimating representative velocity distributions, small extrapolations of the travel time to 30m were used in computing the average velocities. The subsequent analysis of the shallow velocities in this paper make no use of such extrapolations. Fitting travel-time curves to the observed travel times gives average velocities of 618 m/s and 306 m/s for rock and soil boreholes, respectively.

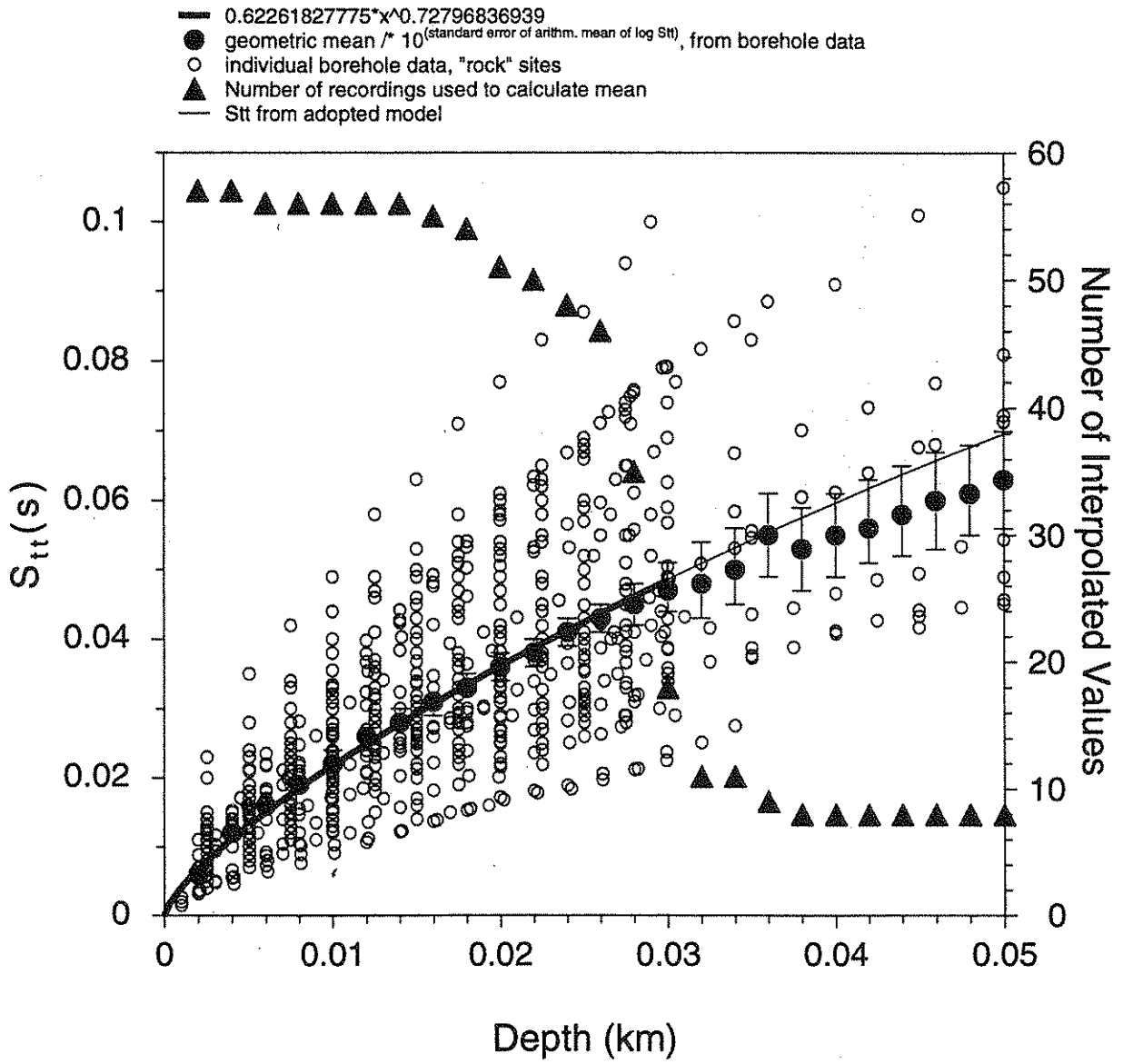

Figure 2. S-wave travel time vs. depth (left axis). The circles are the individual observations, and the solid dots are the geometric means of the interpolated travel times, with standard error of the mean indicated by the error bars. The least-squares fit of a power law is given by the heavy line ($S_{tt} = 0.623z^{0.728}$), and the travel time corresponding to the adopted velocity model is given by the light line. The number of interpolated values at each depth is given by the filled triangles (right axis).

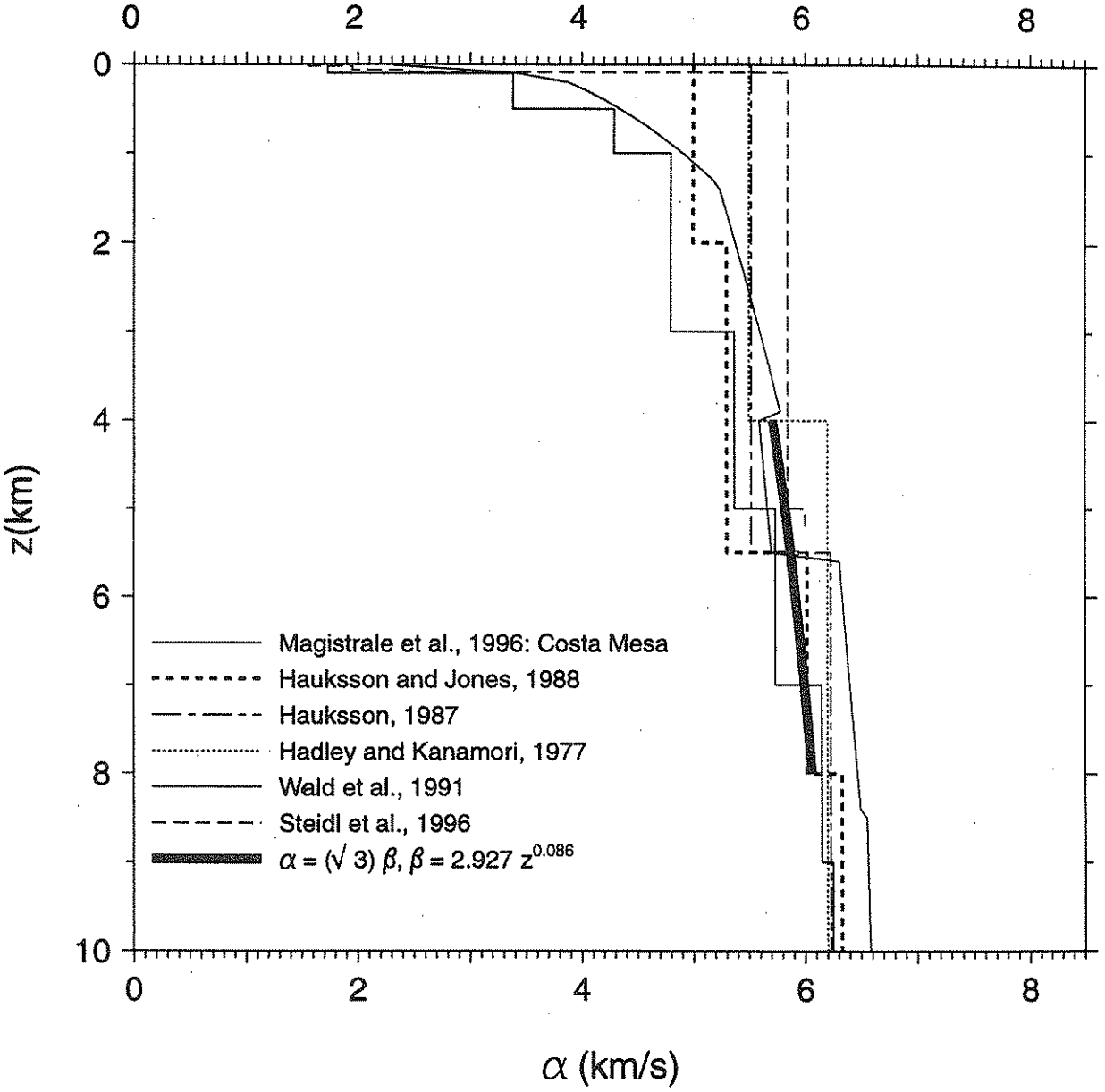

Figure 3. P-velocity vs. depth to 10 km. The heavy line is obtained by multiplying the generic rock shear velocities used in this paper by $\sqrt{3}$; this assumes a Poisson's ratio of 0.25, which we realize is much too small for shallow depths. The intent of this figure is to compare the final velocity profile used in the amplification calculation (heavy line) with various P-velocity profiles at depths greater than several kilometers, where we expect Poisson's ratio to be close to 0.25. The Magistrale *et al.*, 1996, curve is for a point at 33.64° N and 117.93° W.

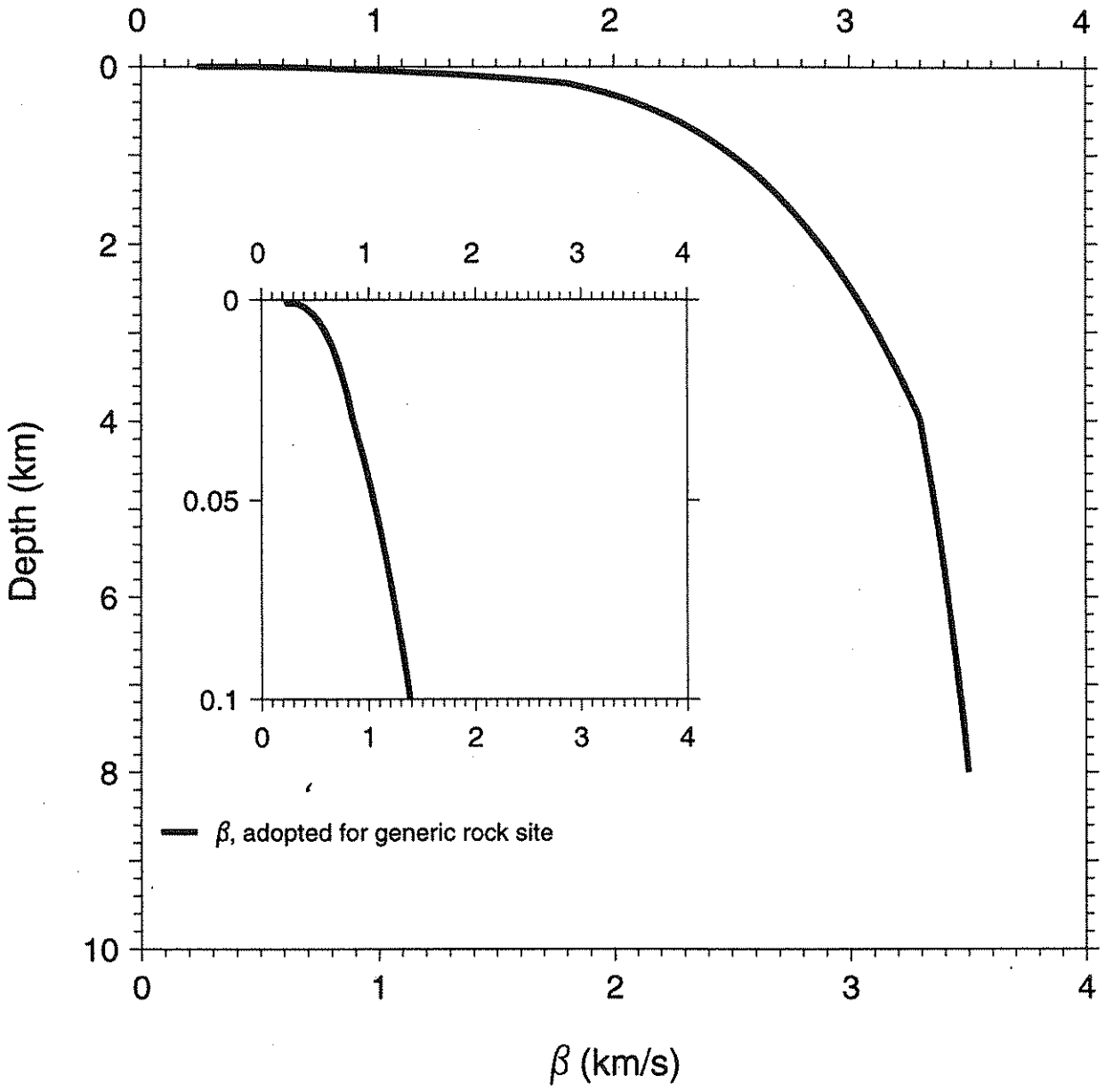

Figure 4. S-velocity vs. depth adopted in this paper for generic rock sites.

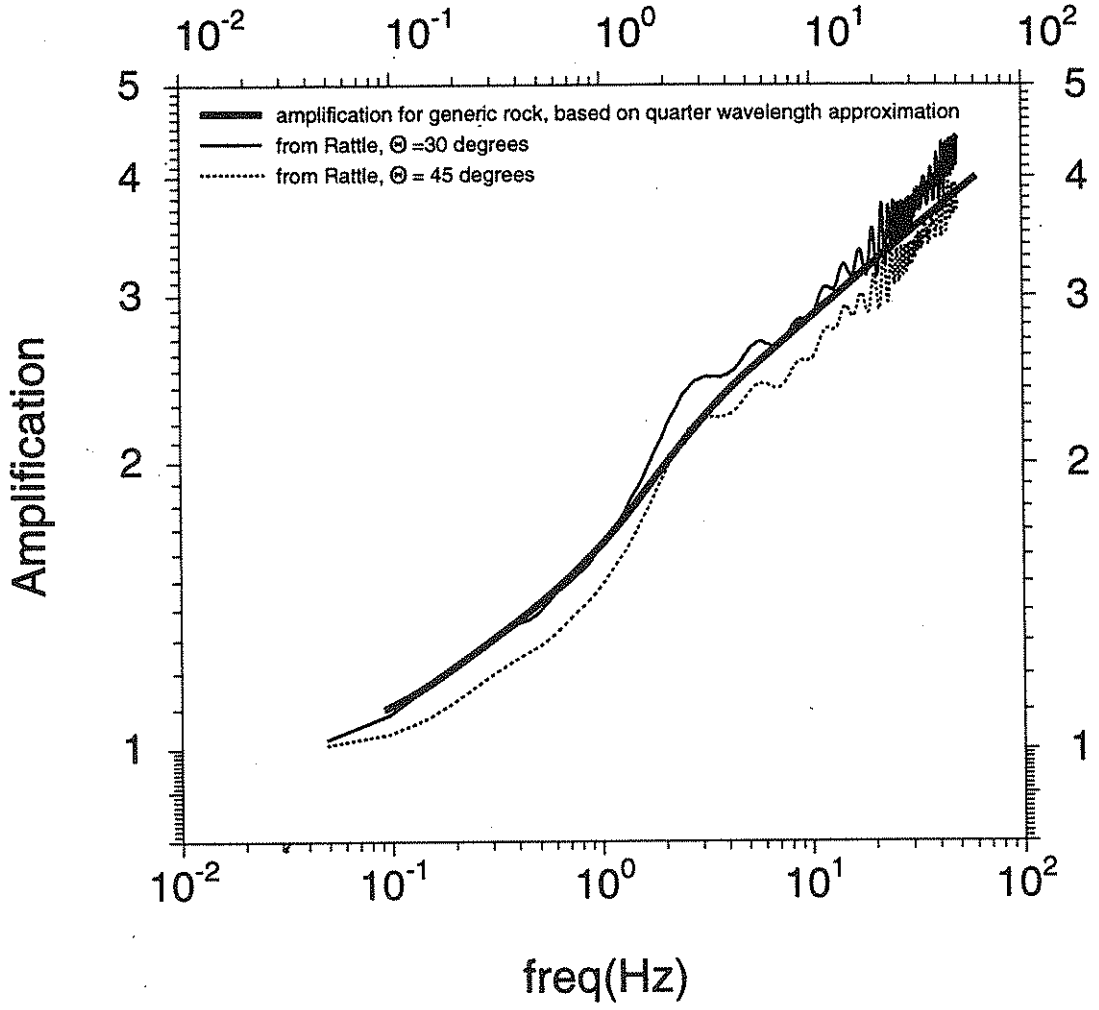

Figure 5. Amplification vs. frequency. The solid line is computed using the quarter-wavelength approximation and the velocity profile shown in Figure 4. The results from plane SH waves incident at the base of a 8-km thick stack of constant-velocity layers (with $Q = 10000$) closely approximating the adopted continuous shear-wave velocity are shown by the light lines for angles of incidence of 30 and 45 degrees; the results were computed from the Haskell matrix method, as implemented by program *Rattle* by C. Mueller.

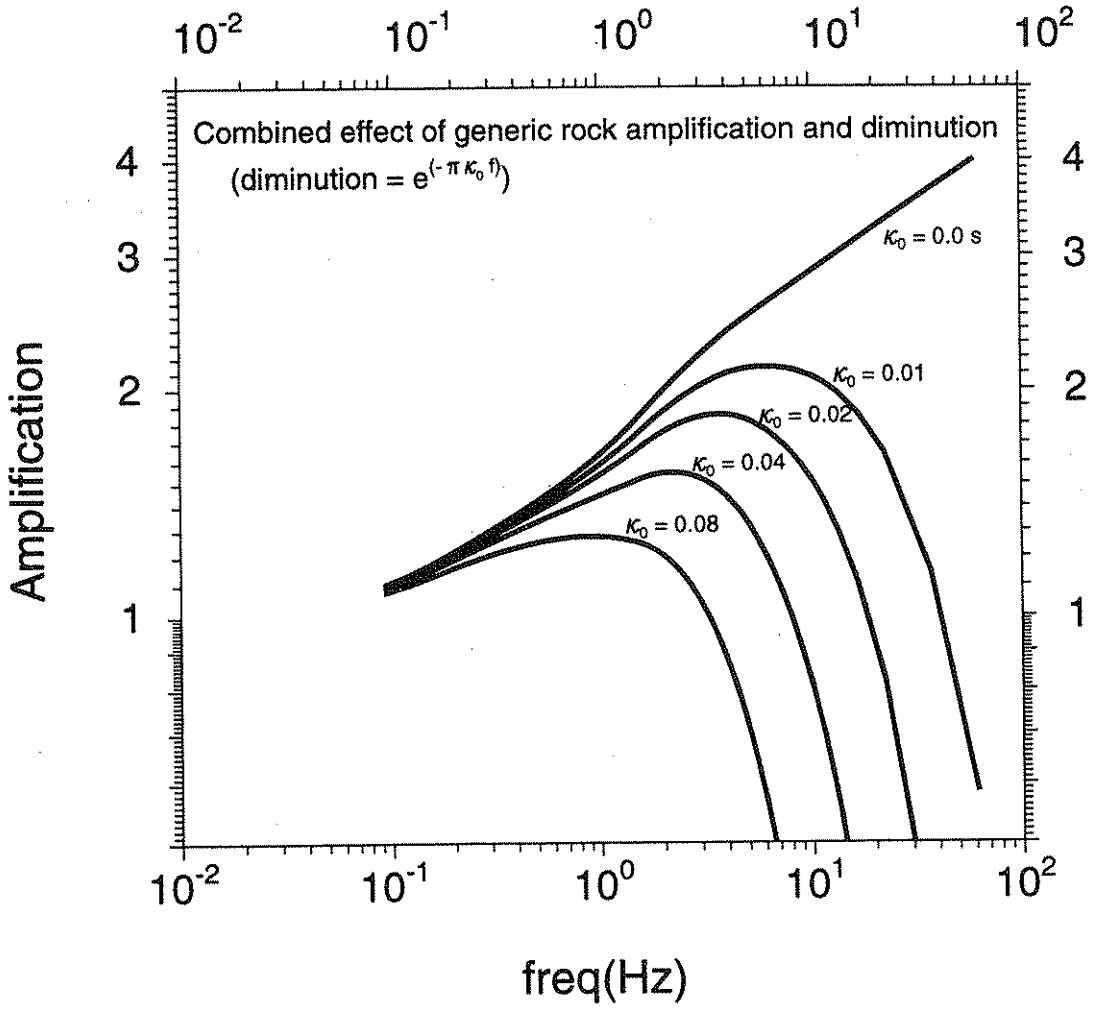

Figure 6. The combined effect of the generic rock amplification given in Figure 5 and the attenuation given by $\exp(-\pi\kappa_0 f)$.

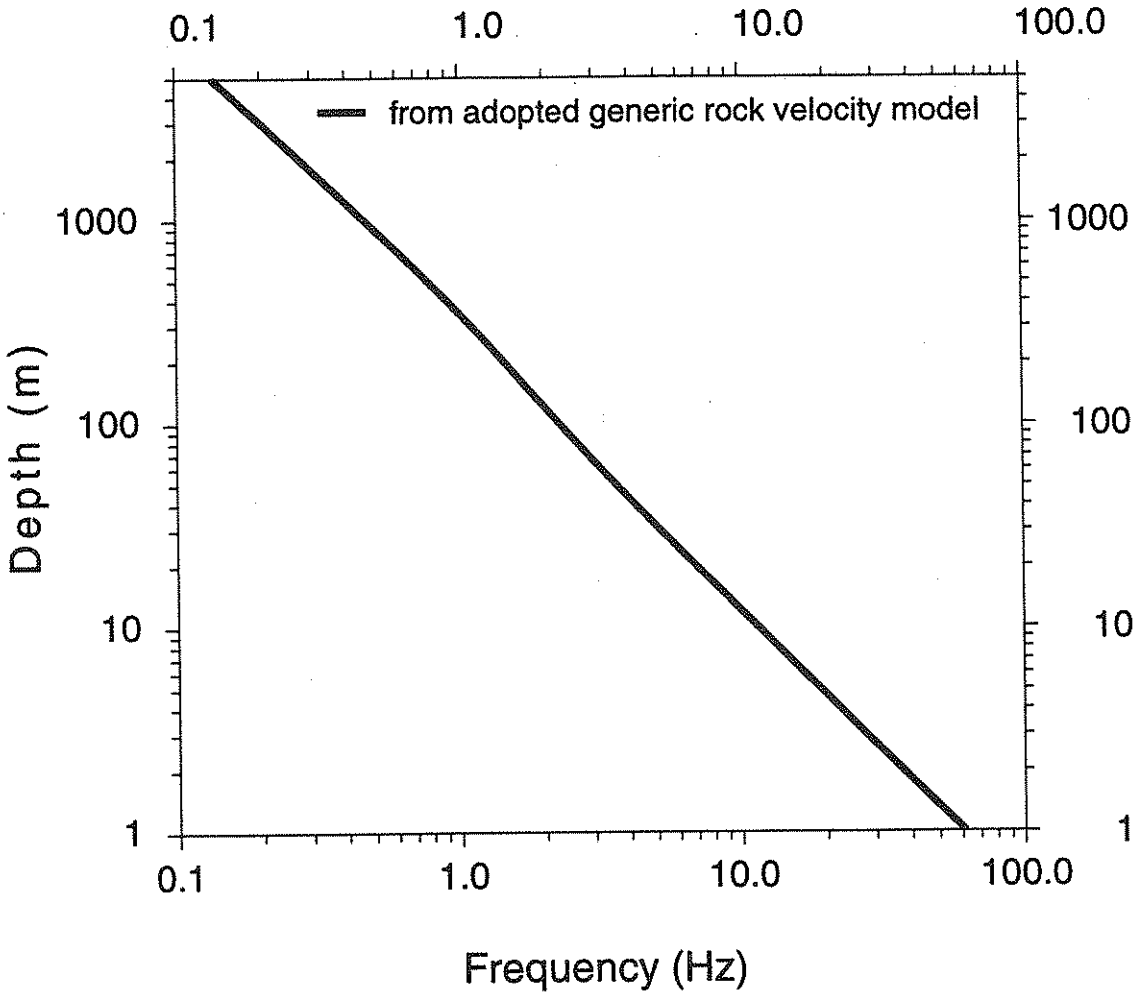

Figure 7. The depth corresponding to a quarter wavelength as a function of frequency for the adopted rock shear-wave velocity model. This figure provides a rough idea of what depths influence what frequencies in the site response.

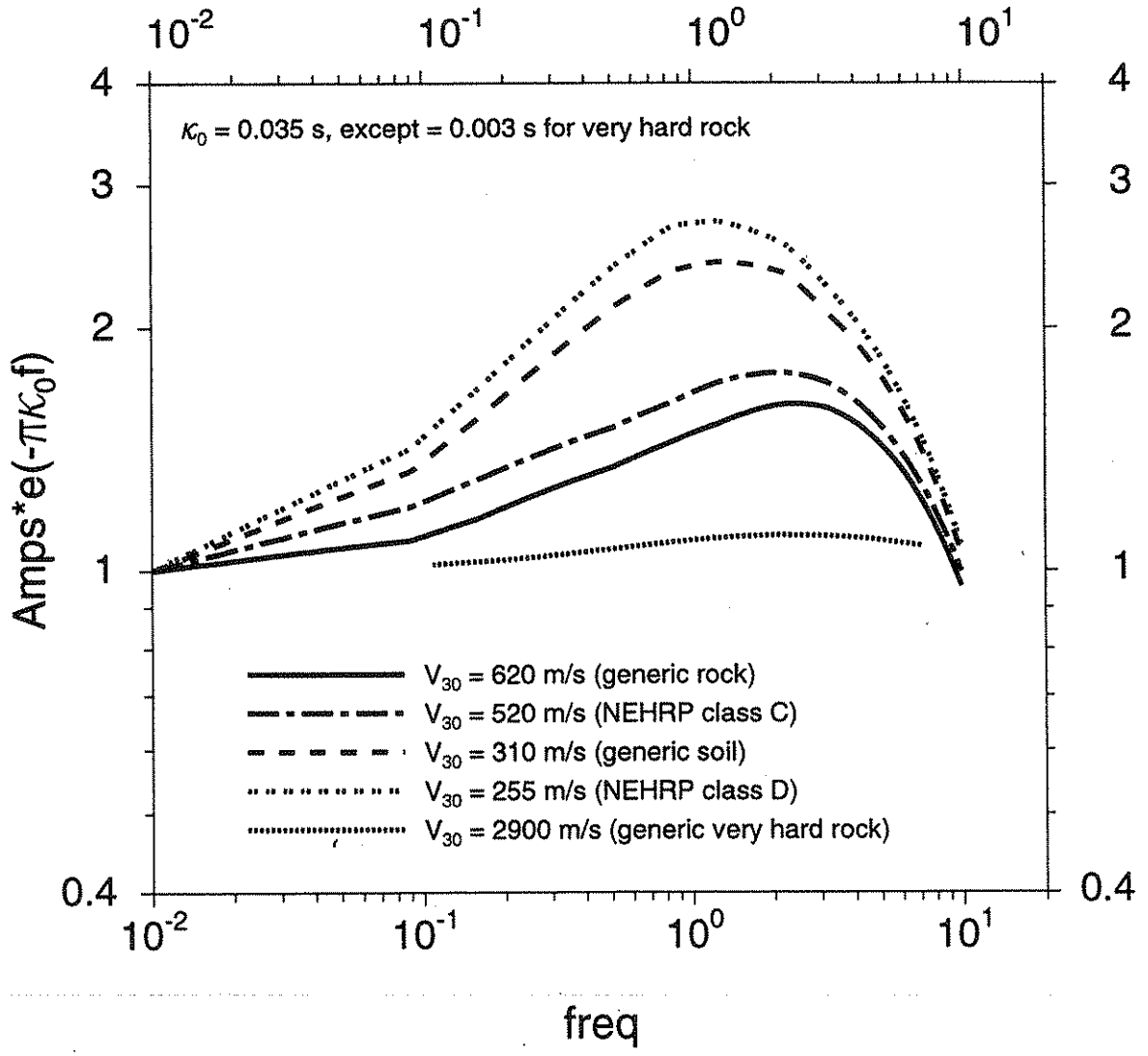

Figure 8. The product of Fourier spectral amplifications and the diminution factor $\exp(-\pi\kappa_0 f)$ for various site conditions, as measured by the average shear-wave velocity in the upper 30 m. The diminution factor used $\kappa = 0.035$ s for all cases except the very hard rock case, for which $\kappa = 0.003$ s.